Pharm Res (2011) 28:1591–1605
DOI 10.1007/s11095-011-0393-x

RESEARCH PAPER

High-Throughput Screening of Excipients Intended to Prevent Antigen Aggregation at Air-Liquid Interface

Sébastien Dasnoy • Nancy Dezutter • Dominique Lemoine • Vivien Le Bras • Véronique Préat

Received: 26 October 2010 / Accepted: 3 February 2011 / Published online: 12 March 2011

ABSTRACT

Purpose The aim was to develop a high-throughput screening method compatible with low protein concentrations, as present in vaccines, in order to evaluate the performance of various excipients in preventing the aggregation at air-liquid interface of an experimental recombinant antigen called Antigen 18A.

Methods Aggregation of Antigen 18A was triggered by shaking in a half-filled vial or by air bubbling in a microplate. Size-exclusion chromatography, turbidimetry, Nile Red fluorescence spectroscopy, and attenuated total reflection Fourier-transform infrared spectroscopy were used to assess Antigen 18A aggregation. A high-throughput method, based on tryptophan fluorescence spectroscopy, was set up to screen excipients for their capability to prevent Antigen 18A aggregation at air-liquid interface.

Results While a similar aggregation profile was obtained with both stress tests when using size-exclusion chromatography, spectroscopic and turbidimetric methods showed an influence of the stress protocol on the nature of the aggregates. The high-throughput screening revealed that 7 out of 44 excipients significantly prevented Antigen 18A from aggregating. We confirmed the performance of hydroxypropyl-β-cyclodextrin and hydroxypropyl-γ-cyclodextrin, as well as poloxamers 188 and 407, in half-filled shaken vials.

Conclusions A high-throughput screening approach can be followed for evaluating the performance of excipients against aggregation of a protein antigen at air-liquid interface.

S. Dasnoy • V. Préat (✉)
Louvain Drug Research Institute, Université catholique de Louvain
Unité de Pharmacie Galénique, Avenue E. Mounier 73, UCL 7320
1200 Brussels, Belgium
e-mail: veronique.preat@uclouvain.be

N. Dezutter • D. Lemoine • V. Le Bras
GlaxoSmithKline Biologicals
Rue de l'Institut 89
1330 Rixensart, Belgium

KEY WORDS excipients · fluorescence spectroscopy · high-throughput screening · protein aggregation · vaccines

INTRODUCTION

From manufacturing to patient administration, vaccines may undergo various stress conditions that can impact antigen integrity and therefore vaccine efficacy (1). One major cause of protein instability is the formation of aggregates (2), which may result in a modified immunogenicity profile of the antigen (3). Ensuring antigen integrity is a critical factor that must be taken into account during the development of new vaccine candidates.

Proteins generally exhibit surface activity (4). In the presence of hydrophobic interfaces, they may be prone to denaturation by exposing their hydrophobic core, resulting in self-association and finally aggregation (2). Air-liquid interfaces can be present at different steps of the vaccine life, when mixing in vessels (manufacturing), dispensing in final containers (filling), during drying processes for solid formulations, during agitation for liquid formulations (shipping), and when freeze-dried formulations are reconstituted (handling).

Several proteins have been reported to aggregate at air-liquid interface, e.g. insulin (5–9), growth hormone variants (8,10–16), IgG variants (17–20), recombinant Factor VIII (21) and XIII (22), and IL-2 mutein (23). Various approaches have been used to study this phenomenon: shaking in the presence of headspace (6,7,16–24), vortexing (10,12,13) and nitrogen bubbling (11). Moreover, some excipients were shown to inhibit aggregation at air-liquid interface, such as polysorbate 20 (10,16,18,20), polysorbate 80 (16,17,19,21–23), poloxamer 407 (12), hydroxypropyl-β-cyclodextrin (10,15,19,24), hydroxypropyl-γ-cyclodextrin

(19), arginine (8), lysine (9), aspartic acid (7,9), glutamic acid (7,9), dextrose (6), and dextrates (6). This is only a limited list, and the use of high-throughput screening (HTS) technologies might provide opportunities for evaluating additional excipients.

With the same amount of antigen, an HTS approach offers the advantage to evaluate a larger number of conditions than with the classical analytical methods. HTS technologies have been used in developing stable formulations of monoclonal antibodies (25), therapeutic proteins (26), and vaccines (27). However, sensitivity issues may make some HTS analytical methods incompatible with the low antigen concentrations found in vaccines.

Antigen 18A is a 68-kDa recombinant glycoprotein consisting of 30% hydrophobic amino acid residues including 9 tryptophans. Its mean hydrophobicity index is 0.48 on the Kyte-Doolittle scale (28). Its experimental isoelectric point is 4.4 ± 0.4, as determined by isoelectric focusing. Its melting temperature by differential scanning calorimetry is 56°C. After stability testing of 1 week at room temperature, neither adsorption of native Antigen 18A to the walls of glass vials nor aggregation was noticed.

Antigen 18A was shown to readily aggregate upon gentle shaking in a vial. The aim of this study was to evaluate the performance of various excipients in stabilizing this protein against aggregation at air-liquid interface. We first demonstrated by chromatographic, light scattering and spectroscopic techniques that conformational changes were involved in Antigen 18A aggregation at air-liquid interface. Then we proposed an HTS approach for testing excipients, based on tryptophan fluorescence spectroscopy. The selection of 44 excipients (amino acids, cyclodextrins, sugars, polyols, polymers and surfactants) was based on their presence in marketed parenteral drug products. Data management and analysis were automated to identify hit compounds from the screening. Further, Antigen 18A biological integrity was evaluated in the presence of these excipients in a shaken half-filled vial model.

MATERIALS AND METHODS

Materials

Antigen 18A was produced by GlaxoSmithKline Biologicals (Rixensart, Belgium). This protein was diluted from stock solution to 125 µg/ml in phosphate buffer (NaH_2PO_4/K_2HPO_4) 10 mM, pH 6.8, leading to a concentration equivalent to that in a common vaccine.

L-Arginine, L-aspartic acid, L-histidine, L-isoleucine, L-leucine, L-proline, L-serine, L-threonine and L-valine were purchased from Ajinomoto (Tokyo, Japan). L-alanine was obtained from Amresco (Solon, OH, United States) and L-glycine from Evonik Rexim (Ham, France). Polyethyleneglycol 15 hydroxystearate (*Solutol® HS15*), polyvinylpyrrolidones (PVP) K12 and K17 (*Kollidon®*), poloxamers (PX) 188 and 407 (*Lutrol®*) were gifts from BASF (Ludwigshafen, Germany). D-Mannitol was purchased from Roquette (Lestrem, France), D-sorbitol from Cargill (Minneapolis, MN, United States), sucrose from VWR (Leuven, Belgium), polysorbate (PS) 80 from NOF (Tokyo, Japan) and hydroxypropyl-γ-cyclodextrin (HP-γ-CD, *Cavasol® W8 HP*) from Wacker (Burghausen, Germany). Hydroxypropyl-β-cyclodextrin (HP-β-CD, *Kleptose® HPB*) was a gift from Roquette. Sulfobutylether-β-cyclodextrin (SBE-β-CD, *Captisol®*) was a gift from CyDex Pharmaceuticals, Inc. (Lenexa, KS, United States), polyoxyl 40 stearate (Myrj 52) was obtained from Croda (Goole, United Kingdom) and sodium dioctylsulfosuccinate (sodium docusate) was purchased from Cytec (Woodland Park, NJ, United States). Calcium chloride, magnesium chloride, magnesium sulphate, potassium hydrogenophosphate, ethanol, polysorbate 20, sodium caprylate, trehalose (Calbiochem), polyethylene glycols (PEG) 300, 600, 1,000, 1,500 and 6,000 were obtained from Merck (Darmstadt, Germany). Polyethylene glycols 400, 3,350 and 4,000 were gifts from Sasol (Johannesburg, South Africa). L-Glutamic acid, glycylglycine, L-lysine, *myo*-inositol, Nile Red (Fluka) and sodium dihydrogenophosphate were supplied by Sigma-Aldrich (Saint Louis, MO, United States). 3,3′,5,5′-Tetramethylbenzidine (TNB) was obtained from Biorad (Hercules, CA, United States). All solutions were prepared with water for injection obtained by triple distillation. Excipient solutions were filtered on a 0.22 µm polyether sulfone membrane (Sartolab, Sartorius Stedim, Aubagne, France). All excipients except glycylglycine were of compendial grade or tested following their respective Ph. Eur. monography prior to use. In the next sections, excipient concentrations presented in percentage were prepared on a weight-to-volume (w/v) basis.

Polypropylene (PP) deepwell microplates (Nunc) were obtained from ThermoFisher Scientific (Waltham, MA, United States), ultraviolet (UV)-transparent 96-well acrylic microtiter plates (Costar #3635) from Corning (Corning, NY, United States) and PP clear microplates (Whatman Uniplate) for pH measurement from GE Healthcare (Waukesha, WI, United States). PP troughs of 100 ml and PP disposable tips were purchased from Tecan (Männedorf, Switzerland). Type I glass vials were supplied by Nuova Ompi (Piombino Dese, Italy) and rubber stoppers from West Pharmaceutical Services (Lionville, PA, United States). UV-transparent seals (VIEWseal) were purchased from Greiner Bio-one (Kremsmünster, Austria). Teflon-stoppered 10×2 mm quartz cells were obtained from Hellma (Müllheim, Germany).

Size-Exclusion Chromatography

Size-exclusion high performance liquid chromatography (SEC) measurements were performed on an Agilent 1,200 chain (Santa Clara, CA, United States). A TSKgel PWXL guard column (6 mm ID × 4 cm) was placed in front of a TSKgel G3000PWXL column (7.8 mm ID × 30.0 cm) from TOSOH (Tokyo, Japan) and loaded with a volume of 100 µl. Phosphate-buffered saline (PBS), pH 7.4, was used as mobile phase at a flow rate of 0.5 ml/min. The elution profile was monitored at 213 nm by a diode array detector. Data acquisition and peak integration calculations were performed using the Chemstation (Agilent) software. In preliminary experiments with multi-angle light scattering and refractive index detectors connected in series, the molecular weight of eluted species was determined (data not shown). The main peak of native protein (elution time 13.4 min) was assigned to monomeric species. Higher molecular weight species eluted at 11.5 min were defined as soluble aggregates. The percentage of those two populations was calculated by reporting the integrated peak area values to the total area under the curve recovered for the non-shaken sample. The extinction coefficients of the monomer and soluble aggregates were considered identical. Protein mass recovery was calculated by dividing the sum of monomer and soluble aggregate peak areas by the total area under the curve of the non-shaken sample.

Turbidimetry

Optical density measurements were performed in a quartz cell on a UV-visible spectrophotometer Ultrospec 2100pro (GE Healthcare). Spectra were recorded at room temperature between 200 and 400 nm, at a speed of 1,500 nm/min and with a scanning step of 0.5 nm. The matrix signal (placebo, antigen-free solution) was subtracted. Sample turbidity was assessed at 350 nm (OD_{350}), as the signal at this wavelength is not due to chromophoric absorption but to light scattering.

Right-angle light scattering (RALS) measurements were performed in a quartz cell, on a LS50b spectrofluorometer (Perkin Elmer, Waltham, MA, United States) equipped with a four-cell holder thermostated at 25°C by a water-circulating bath (Julabo, Seelbach, Germany). A scan synchronized in wavelength was performed between 450 and 650 nm. In this configuration, the signal reaching the detector located at 90° only originates from light scattering (29). The excitation and emission slits were both set at 2.5 nm, the scanning step at 0.5 nm and the scanning speed at 1,500 nm/min. Each spectrum was the average of five consecutive scans. The matrix signal was subtracted. A wavelength of 500 nm was selected as a good compromise between sensitivity and signal stability.

Absorption Spectroscopy

Analyses were performed at 25°C on a Varioskan Flash microplate reader (ThermoFisher Scientific, Waltham, MA, United States). The bandwidth and integration time were set at 5 nm and 100 ms, respectively. The matrix signal was subtracted.

Sample pathlength (L) was obtained by measuring the water absorption peak in the near-infrared region at 975 nm, corrected for baseline at 900 nm (30). The obtained value was not classically expressed in length units but as a height of water peak in absorbance units (AU). A dose range experiment with Antigen 18A allowed us to calculate an apparent extinction coefficient at 280 nm (ε) of 7.5 10^{-3} $AU^{-1}.\mu g^{-1}.ml$ in phosphate buffer. The protein chromophoric absorbance at 280 nm (A_{280}) was calculated by measuring the optical density at 280 nm corrected for light scattering at 320 nm. Based on the Lambert-Beer law, sample concentration (C) can be calculated with Eq. 1.

$$C = \frac{A_{280}}{\varepsilon L} = \frac{1}{\varepsilon}\left(\frac{A_{280}}{A_{975}}\right) = \frac{1}{\varepsilon}\left(\frac{OD_{280} - OD_{320}}{OD_{975} - OD_{900}}\right) \quad (1)$$

Compared with classical absorbance measurements in spectroscopic cells, sample composition may influence the meniscus shape and therefore the pathlength and apparent extinction coefficient. For this reason, this technique was only used for following variations in protein concentration on a well-to-well basis.

Tryptophan Fluorescence Spectroscopy

Measurements were performed at 25°C in a Varioskan Flash microplate reader (ThermoFisher Scientific). While a higher signal-to-noise ratio was obtained by exciting Antigen 18A at its wavelength of maximum absorption (282 nm), a selective excitation of tryptophan residues at 295 nm (29) showed a higher repeatability in preliminary studies (data not shown). The excitation and emission wavelengths were 295 nm and 336 nm, respectively. The excitation slit was set at 12 nm and the integration time at 500 ms. Bottom optics were used to be independent of sample volume variations.

Nile Red Fluorescence Spectroscopy

Nile Red emission and anisotropy were measured. Preliminary studies showed that no inner filter effect was observed at the dye concentration used in both techniques. Emission measurements were performed in microplate at 25°C in a Varioskan Flash microplate reader (ThermoFisher Scientific) equipped with an automated dispenser. The sample initial volume was 150 µL, to which 2 µL of Nile Red from a 100 µM ethanolic solution were added with the primed

dispenser, leading to a final concentration of 1.3 µM Nile Red in solution. The plate was shaken at 300 rpm during 30 s and left at room temperature for 5 min prior to starting analysis. The excitation wavelength was set at 575 nm and the excitation slit at 12 nm. Emission scans were recorded between 600 and 700 nm, with a scanning step of 1 nm and an integration time of 500 ms. The top optics were used. In preliminary trials, we verified that neither the presence of Nile Red nor the sample preparation impacted the protein conformation (tryptophan fluorescence) and aggregation state (optical density). Raw scan values were exported for subsequent spectral processing and analysis with customized macros developed in Visual Basic (Microsoft, Redmond, WA, United States). Both the matrix signal in the presence of Nile Red and the light scattering contribution from dye-free samples were subtracted. Difference spectra were obtained by subtracting the spectrum of the non-stressed sample from the spectra of stressed samples and revealed that main changes in intensity occurred at 625 nm. This wavelength was selected for studying variations in fluorescence intensity. Spectra were first smoothed with a seven-points filter and third degree Savitky-Golay polynomial and then the intensity at 625 nm extracted. The centre of gravity of the emission ($\langle\lambda\rangle$) was calculated by the centre of spectral mass position ($\overline{\nu}_{csm}$) method (Eq. 2). Bandpass correction was applied when converting intensities (I) from wavenumbers ($\overline{\nu}$) to wavelength (λ) units (29). No smoothing was required, as the noise regular pattern has a low impact on the centre of spectral mass position. Compared with the emission wavelength of maximum intensity, this approach does not involve any mathematical transformation of raw data and allows a better detection of subtle changes in the spectral shape.

$$\langle\lambda\rangle = \frac{1}{\overline{\nu}_{csm}} = \frac{\sum I(\overline{\nu})}{\sum \overline{\nu} I(\overline{\nu})} = \frac{\sum \lambda^2 I(\lambda)}{\sum \lambda I(\lambda)} \quad (2)$$

Anisotropy measurements were performed in a quartz cell, on a LS50b spectrofluorometer (Perkin Elmer) equipped with a four-cell holder thermostated at 25°C by a water-circulating bath (Julabo). Just prior to analysis, 5 µL Nile Red from a 100 µM ethanolic solution were added to 495 µL sample, leading to a final dye concentration of 1 µM. The cell content was homogenized by gentle mixing. The excitation wavelength was set at 575 nm, the slits at 15 nm (excitation) and 20 nm (emission), the scanning step at 0.5 nm and the scanning speed at 300 nm/min. For each sample, four different spectra were recorded from 600 to 625 nm with the following excitation/emission polarizer combinations: I_{hh}, I_{vv}, I_{hv} and I_{vh}. Indices are related to horizontal (h) and vertical (v) positions. Each spectrum was the average of five consecutive scans. Anisotropy spectra were obtained by calculating anisotropy (r) at each wavelength (Eq. 3) (29):

$$r = \frac{I_{vv} - GI_{vh}}{I_{vv} + 2GI_{vh}}, \text{ with } G = \frac{I_{hv}}{I_{hh}} \quad (3)$$

Difference spectra revealed that the main changes in anisotropy occurred at 605 nm. This wavelength was selected for studying variations in fluorescence anisotropy. In preliminary studies, we observed that the present scanning approach allowed us to get more repeatable results than a direct measurement of anisotropy at 605 nm.

ATR-FTIR Spectroscopy

Samples were analyzed on a Tensor 27 Fourier-transform infrared (FTIR) spectrometer equipped with an attenuated total reflection (ATR) module (Bruker, Ettlingen, Germany). The detector was cooled with liquid nitrogen and the chamber purged with dry air. Each spectrum was the average of 256 scans recorded from 4,000 to 400 cm^{-1}. A sample volume of 3 µL was poured onto the ZnSe crystal, and water was evaporated by flushing with dry nitrogen. The effect of adsorption to ZnSe crystal on Antigen 18A conformation was not evaluated. Each sample was analyzed in triplicate. A baseline was recorded before each triplicate measurement. Based on a Student's statistical test (α=0.01), the Kinetics application (31) was used to highlight significant differences in the Amide I (1,710–1,600 cm^{-1}) region that is known to be sensitive to protein secondary structure (carbonyle stretching). The OPUS software (Bruker) was used for data acquisition, subtraction of matrix signal, averaging of triplicate spectra and offset correction. Spectra were exported for subsequent processing with customized macros developed in Visual Basic (Microsoft). After a linear baseline correction, the second-derivative spectra were calculated with a nine-points filter and second degree Savitky-Golay polynomial, smoothed with the same polynomial and then vector-normalized in the Amide I region. The similarity between second-derivative spectra was studied by the area of overlap method (32).

Enzyme-Linked Immunosorbent Assay

A direct sandwich enzyme-linked immunosorbent assay (ELISA) method was applied to evaluate the integrity of Antigen 18A epitopes. Antigen 18A samples were incubated overnight in the presence of an excess of primary polyclonal antibody (commercial source). The samples were transferred in microplates (MaxiSorp, Nunc, ThermoFisher Scientific) coated with a defined quantity of Antigen 18A before the secondary antibody coupled with peroxidase

(Sigma-Aldrich) was added. After addition of the peroxidase substrate (TMB), the intensity of the colorimetric reaction was measured in a spectrophotometer (Versamax, Molecular Devices, Sunnyvale, CA, United States) at 450 and 620 nm. The calibration curve was fitted to a sigmoid by the four-parameter method in the SoftMax Pro software (Molecular Devices), and allowed the calculation of the concentration of native Antigen 18A.

High-Throughput Screening

A series of 44 excipients were evaluated at six different concentrations in triplicate. For each condition, a single placebo was prepared and used as a blank to be subtracted in spectroscopic analyses. In preliminary studies, variability in edge wells was 2% higher than in inner wells. The outer rows were reserved for blanks. On each plate, one well by row was dedicated to the excipient-free control sample (inner rows, six wells) or its associated blank (outer rows, two wells).

The screening was performed on a total of 12 plates. A customized application developed in Visual Basic (Microsoft) randomized all conditions and generated XML worklists containing liquid volumes to be added in each well. Replicates were located on different plates.

All samples contained phosphate buffer (NaH_2PO_4/K_2HPO_4) 10 mM, pH 6.8. The stock solution concentrations were the following: 100 mM phosphate buffer, 0.5% surfactants, 3% polymers, 15% polyols except 12% inositol, 15% carbohydrates and cyclodextrins, 10 mM calcium and magnesium salts, 250 mM sodium chloride, 3 mM aspartic acid, 50 mM glutamic acid, 150 mM leucine, 250 mM isoleucine and 500 mM other amino acids.

Based on the XML worklists processed by a Visual Basic application (Microsoft) and subsequently imported into the Gemini software (Tecan), a Genesis liquid handling station equipped with an eight-tip liquid handling (LiHa) arm (Tecan) prepared excipient mixes at a volume of 1,000 µL in deepwell microplates.

The transfer from deepwell to microtiter plates was performed with a 96-channel head (TeMo) equipped with disposable tips (Tecan). From a deepwell stock plate, the antigen or equivalent buffer volume was added to the microtiter plates with the TeMo. Two microtiter plates were prepared from a deepwell microplate, one for air-bubbling stress test and the other for pH check. The air-bubbling and pH plates were filled with 150 µL/well and 200 µL/well, respectively. In the latter, pH measurement was automatically performed in each well with a probe adapted to a MiniPrep station (Tecan).

The air-bubbling plates were analyzed by ultraviolet spectroscopy and tryptophan fluorescence spectroscopy before and after stress test. A custom application developed in Visual Basic (Microsoft) allowed processing and analysis of data generated from the HTS study, as such identifying hit conditions with a statistical approach.

Air-Liquid Interface Stress Test

The behaviour of Antigen 18A at the air-liquid interface was studied in vials closed with rubber stoppers and sealed with aluminium crimps. The vials were filled at half (1.5 ml) or at maximum (3.625 ml as determined by weighing) volume. Then they were tape-fixed horizontally on an agitating plate and shaken at 200 rpm. During kinetics studies, vials were picked up randomly every 15 min for analysis.

In microplate, air bubbling was performed with the TeMo head. A series of air bubbles (30 µL) was blown in each well, with a periodicity of 1 min. After this stress test, microplates were sealed and centrifuged during 5 min at 1,000 rpm for eliminating residual air bubbles. Preliminary tests showed that centrifugation did not impact the spectroscopic measurements.

Statistical Analysis

Parametric tests are based on sample independence, normality and homoscedasticity assumptions. Raw data were first analyzed by the Box-Cox method in Design Expert (Stat-ease, Minneapolis, MN, United States) in order to test if power or logarithmic transformations are able to improve the normality profile of the residuals frequency distribution. In case a transformation was identified, it was applied to the data. All subsequent calculations were performed with the Unistat Excel add-in (Unistat, London, United Kingdom). The normality hypothesis was verified by the Shapiro-Wilk test. Moderate non-normality was accepted in case the skewness [−1.5;1.5] and kurtosis [−1;2] values were not too far from the null value (33). The homogeneity of variance hypothesis was evaluated by the Cochran test. After verification of normality and homoscedasticity conditions, an analysis of variance (ANOVA) followed by a Dunnett test approach was adopted. All statistical tests were performed with a risk factor $\alpha = 5\%$. In the HTS study, the ANOVA-Dunnett approach ($\alpha = 1\%$) was adapted to automation in Visual Basic (Microsoft).

The HTS study encompassed 72 excipient-free controls (six by plate) that allowed us to determine the repeatability (intraplate), reproducibility (interplate) and global variability (intraplate + interplate) of the screening. These parameters were calculated based on an ANOVA approach.

The z'-value is a common adimensional parameter used for evaluating the quality of an HTS assay. Based on the mean (μ) difference and variability (σ) of positive ($C+$) and

negative (*C–*) controls, a separation band was calculated, based on Eq. 4. The identification of hits by an HTS method is considered as feasible when z'-values are greater than or equal to 0.5 (34).

$$z' = 1 - 3\frac{(\sigma_{C+} + \sigma_{C-})}{|\mu_{C+} - \mu_{C-}|} \quad (4)$$

RESULTS

Aggregation Kinetics in a Shaken Vial

The influence of an air-liquid interface on Antigen 18A aggregation kinetics was studied by filling vials with different volumes of protein solution. Vials were tape-fixed horizontally on an agitating plate and shaken during 5 h 45 min, in the presence (half volume) or absence (maximum volume) of air-liquid interface. The non-shaken sample was used as a reference for statistical analyses.

The protein aggregation kinetics during shaking were followed by SEC (Fig. 1). In half-filled vials only, the monomer gradually degraded while soluble aggregates formed. Significant differences with the control were detected in both populations from 1 h of shaking ($p<0.05$). A significant loss in protein mass recovery was observed from 3 h 30 min of shaking ($p<0.05$).

Whatever the filling volume in vials, no change in turbidity was detected by visual inspection during the whole experiment. However, in half-filled vials, an increase in turbidity with shaking time was observed from 2 h 15 min by right-angle light scattering and from 3 h 30 min by optical density ($p<0.05$) (Fig. 2).

The influence of shaking on Antigen 18A tertiary structure was followed by tryptophan fluorescence spectroscopy. No significant change ($p>0.05$) in tryptophan emission was observed (data not shown).

Shaking-induced conformational changes of Antigen 18A were observed in half-filled vials by Nile Red fluorescence spectroscopy (Fig. 3). For thermodynamic reasons, hydrophobic regions generally are barely exposed to water when proteins are in their native conformation. When a protein denatures or unfolds, hydrophobic patches may become more exposed to the solvent. Changes in protein surface hydrophobicity, associated with protein denaturation and aggregation can be detected by an increased affinity for Nile Red, a non-ionic hydrophobic fluorescent dye (35,36). Recently, this technique was used in high-throughput protein formulation screening (26). Upon shaking in half-filled vials, we observed ($p<0.05$) an increase in Nile Red fluorescence intensity from 1 h 30 (Fig. 3b), a blue-shift in the center of gravity of emission from 30 min (Fig. 3c), and an increase in anisotropy from 1 h (Fig. 3d). Those parameters reflect a change in the environment of the dye molecules: increase in hydrophobicity (intensity) and polarity (blue-shift), as well as decrease in mobility (anisotropy) (29).

The protein secondary structure of Antigen 18A was also modified by shaking vials in the presence of air-liquid interface, as evidenced by changes in the Amide I region of ATR-FTIR spectra (Fig. 4a). The relative contribution of absorbing species was studied, based on vector-normalized second-derivative spectra (Fig. 4c). The native structure was characterized by a main peak at 1,637 cm^{-1} that we assigned to the presence of β-sheet. Three other minor peaks were attributed to β-sheet or turns (1,668 cm^{-1} and 1,686 cm^{-1}), and α-helix or random coil structures

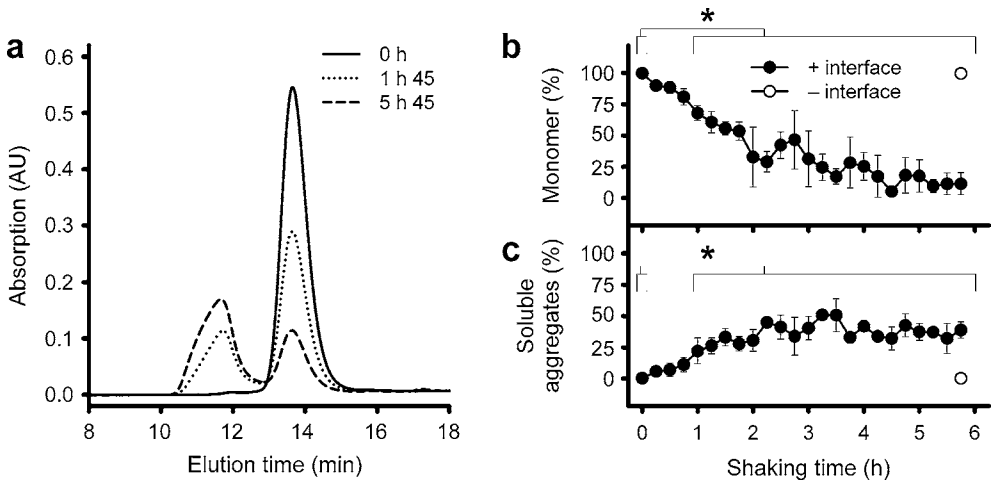

Fig. 1 Influence of air-liquid interface on Antigen 18A aggregation profile by size-exclusion chromatography, in a shaken vial model. (**a**) Chromatograms (UV signal at 213 nm) obtained from a half-filled vial before (0 h) and after shaking (1 h 45 min and 5 h 45 min). The matrix signal was subtracted. Evolution of monomer (**b**, elution time: 13.4 min) and soluble aggregates (**c**, elution time: 11.5 min) during shaking of vials filled at half and maximum volume. *Error bars* represent the standard deviation from three independent experiments. In the presence of interface, the *star symbol* indicates significant difference with the non-shaken control ($p<0.05$) by ANOVA-Dunnett analysis.

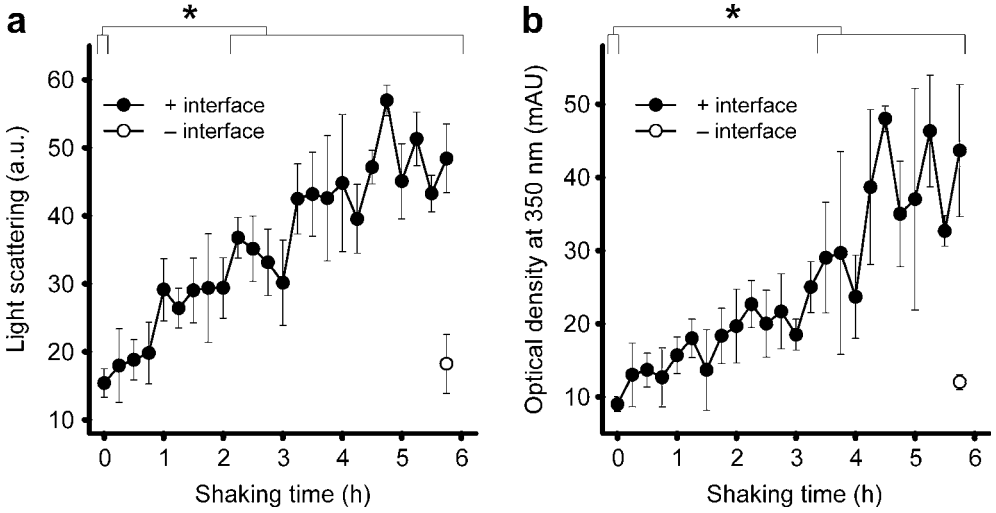

Fig. 2 Influence of air-liquid interface on Antigen 18A aggregation by right-angle light scattering at 500 nm (**a**) and optical density at 350 nm (**b**), in a shaken vial model. *Error bars* represent the standard deviation from three independent experiments. In the presence of interface, the *star symbol* indicates significant difference with the non-shaken control ($p < 0.05$) by ANOVA-Dunnett analysis.

(1,652 cm^{-1}) (37,38). The minor peak detected at 1,700 cm^{-1} was not attributed. During shaking, all these peaks gradually disappeared, and a large peak ($p<0.01$) concomitantly appeared at 1,632 cm^{-1}, which was assigned to β-sheet. In zero-order spectra, reorganization in the β-sheet region was reflected by the 1,632/1,637 cm^{-1} ratio that increased from 1 h 15 ($p<0.05$) (Fig. 4b). A loss in spectral similarity was noticed (Fig. 4d). Taken as a whole,

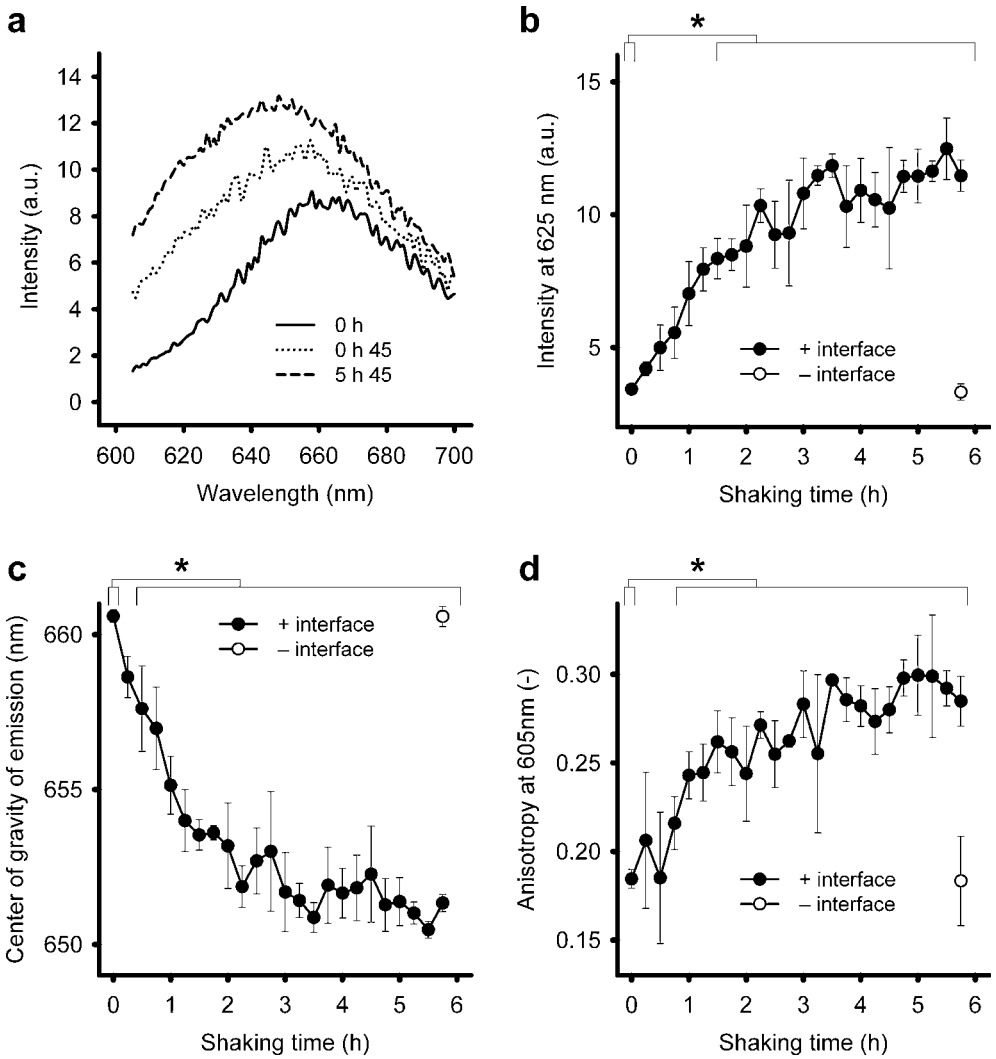

Fig. 3 Influence of air-liquid interface on Antigen 18A surface hydrophobicity by Nile Red fluorescence spectroscopy, in a shaken vial model. Emission scans (**a**) obtained from a half-filled vial before (0 h) and after shaking (0 h 45 min and 5 h 45 min), from which intensity at 625 nm (**b**) and the centre of gravity of emission (**c**) are extracted. Evolution of anisotropy at 605 nm (**d**) upon shaking. *Error bars* represent the standard deviation from three independent experiments. In the presence of interface, the *star symbol* indicates significant difference with the non-shaken control ($p < 0.05$) by ANOVA-Dunnett analysis.

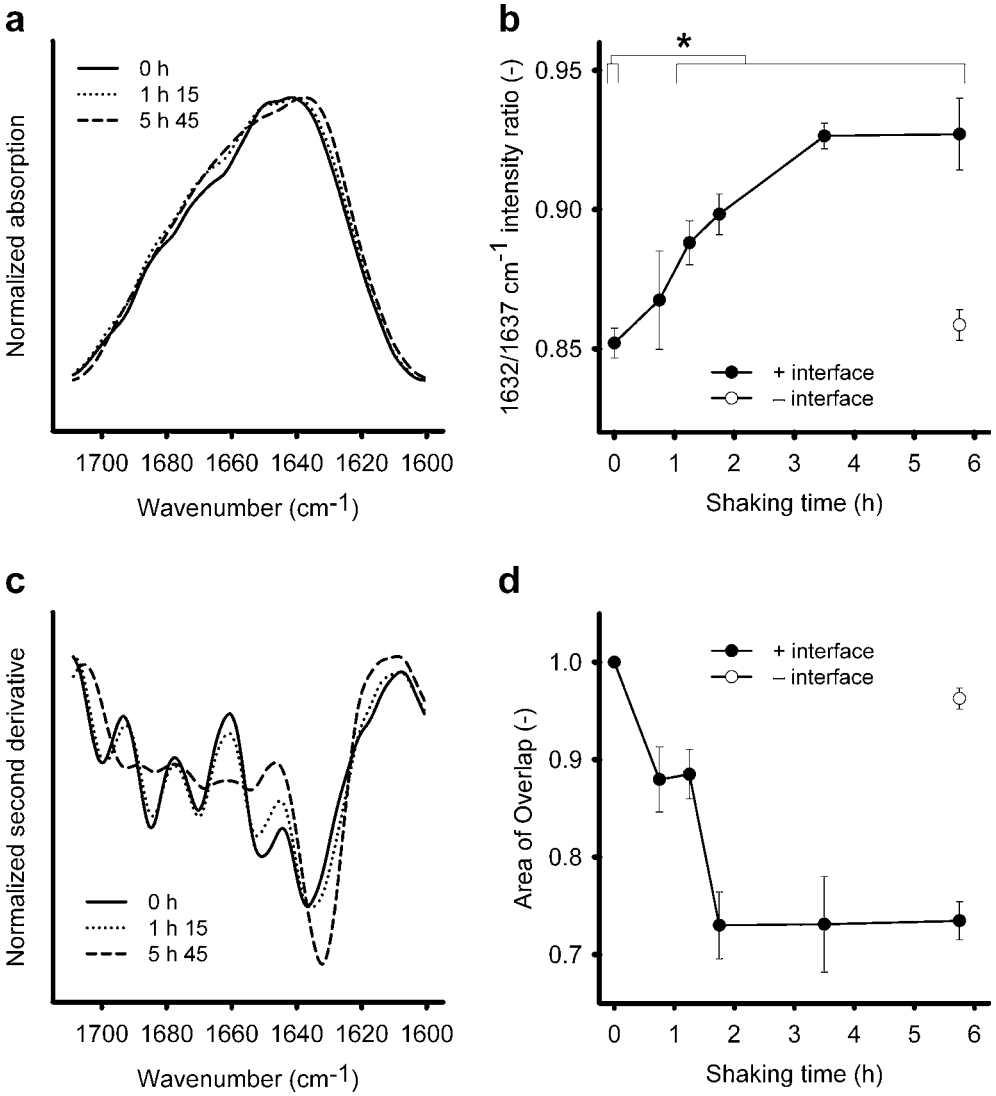

Fig. 4 Influence of air-liquid interface on Antigen 18A secondary structure by attenuated total reflection Fourier-transform infrared spectroscopy, in a shaken vial model. Normalized absorption spectra (**a**) obtained from a half-filled vial before (0 h) and after shaking (1 h 15 min and 5 h 45 min) from which the 1,632/1,637 cm^{-1} intensity ratio is extracted (**b**). Vector-normalized second-derivative spectra (**c**) from which the area of overlap is calculated (**d**). *Error bars* represent the standard deviation from three independent experiments. In the presence of interface, the *star symbol* indicates significant difference with the non-shaken control ($p < 0.05$) by ANOVA-Dunnett analysis. The intrinsic normalization of area of overlap precluded a statistical comparison to the non-shaken sample.

we observed an increase of the relative contribution of β-sheet structures with shaking time in half-filled vial.

In conclusion, Antigen 18A structural stability was studied upon shaking in the presence or absence of air-liquid interface. After 5 h 45 min of shaking, changes in Antigen 18A aggregation profile, tertiary and secondary structure ($p<0.05$) due to the air-liquid interface were emphasized with a combination of chromatographic, light scattering and spectroscopic techniques.

Aggregation Kinetics in a Microtiter Plate

In order to protect Antigen 18A against aggregation at air-liquid interface, we aimed at developing an HTS approach for rapidly evaluating the performance of a large number of excipients.

The first step was to develop a stress test in microplate to follow protein aggregation at air-liquid interface. After unsuccessful trials to aggregate Antigen 18A by plate shaking or vortexing, air-liquid interface was created in wells by air bubbling. Basically, air was first aspirated in tips mounted on a 96-channel head and then blown synchronously in all the wells of a microplate. As polysorbate 80 solutions rapidly foam up upon air bubbling, we used this surfactant for optimizing the liquid volume in the wells, the volume of air bubbles and their periodicity. With a well-filling volume of 150 µl, well-to-well contamination was successfully avoided by leaving a break time of 1 min between air bubbles of 30 µl.

Once the stress test parameters were set up, Antigen 18A aggregation kinetics upon air bubbling was followed in the microplate by tryptophan fluorescence and ultraviolet absorption. No change in turbidity was noticed, as evaluated by optical density measurement at 350 nm. In parallel with these label-free methods, the aggregation profile was measured by size-exclusion chromatography.

A change in fluorescence intensity can be attributed to a conformational change only when the sample concentration

remains stable during the stress test. However, during air bubbling, water evaporation or material loss by adsorption on tips may occur. As a consequence, well-to-well variations in protein concentration may lead to misinterpretations of tryptophan fluorescence data, and this should be avoided. The interchangeability of ultraviolet absorption and tryptophan fluorescence for measuring the concentration of native Antigen 18A was first verified (Fig. 5). It was also observed that absorption spectroscopy is a more reliable method than fluorescence spectroscopy for determining protein content in the presence of aggregated species (data not shown). Indeed, absorption is a faster process than fluorescence; it is less sensitive to solvent polarity hence to protein conformation (29). Therefore, the concentration dependence of tryptophan fluorescence was suppressed by normalizing all results with protein concentration determined by ultraviolet absorption (39). Both measurements were successively performed on each well in the same microplate reader.

Antigen 18A aggregation state was reproducibly controlled by adapting the number of air bubbles used in the test (Fig. 6a). A good correlation was observed between monomer detected by SEC and tryptophan fluorescence intensity (Fig. 6b). In order to have a reasonable stress test with an acceptable variability, we decided to set up the number of air bubbles at 100, corresponding to 44±2% monomer loss.

High-Throughput Screening of Excipients

The development of the microplate-adapted stress test for studying Antigen 18A aggregation at air-liquid interface made possible an HTS of excipients by tryptophan fluorescence spectroscopy.

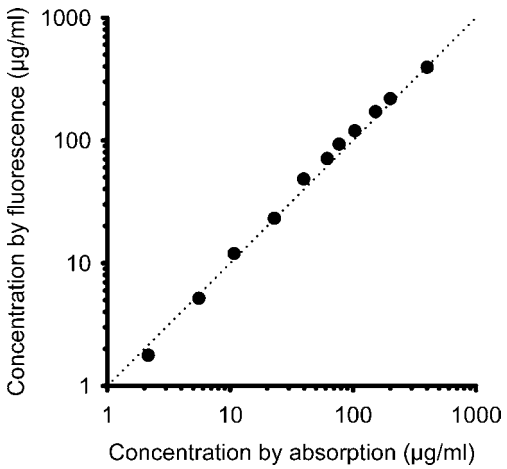

Fig. 5 Comparison of ultraviolet absorption spectroscopy and tryptophan fluorescence spectroscopy in determining the concentration of native Antigen 18A in microplate.

A panel of 44 excipients was investigated. Since an HTS approach allows the testing of a large number of conditions, this selection encompassed compounds from various chemical natures, independently of their described mode of action. The only selection criterion of an excipient was its presence in at least one marketed parenteral product. The working concentrations of excipient families were based on their usual injectability range. However, some amino acids (aspartic acid, glutamic acid, leucine and isoleucine) were tested at lower concentrations due to solubility issues at the target pH (6.8) of the study. Before screening, no interference of excipient stock solutions was noticed by both ultraviolet absorption and tryptophan fluorescence.

The performance of these 44 excipients was evaluated in triplicate at six different concentrations. The entire screening consisted of 12 plates in which all conditions were randomized. Excipient-free controls were present on each plate. More details can be found in the Materials and Methods section.

Sample preparation was performed with an automated liquid handler. Each plate was analyzed, submitted to air bubbling, centrifuged and analyzed again. A customized application was designed for data management and analysis. For each well, sample concentration was obtained from ultraviolet absorption spectroscopy. In excipient-free controls, we observed a decrease in protein concentration of 36±9% due to air bubbling, even if 30±4% water evaporation (30) was measured. We hypothesize that protein loss occured by adsorption on tips or on the walls of microplate wells. In the presence of excipients, a decrease in protein concentration was noticed in 42% of the wells, suggesting that 58% of these conditions inhibited protein loss by adsorption. The change in tryptophan fluorescence intensity normalized for concentration was then computed (F/F_0). This parameter was used for evaluating protein conformational change upon air bubbling in the presence of excipients. Based on an ANOVA followed by a Dunnett test ($\alpha=0.01$), a statistical module automatically evaluated if each condition (three samples) was significantly different from excipient-free controls (72 samples).

Results of the screening are presented in Fig. 7. The conditions where significant protection or destabilization of Antigen 18A was observed are labelled with black-filled or grey-filled symbols, respectively. Interestingly, different patterns were observed when studying the effect of excipient concentration on tryptophan fluorescence intensity. For instance, a linear increase was obtained for hydroxypropyl-cyclodextrins, a bell-shaped curve for poloxamers and a U-shaped curve for polyvinylpyrrolidones.

Among the 44 excipients evaluated, hit compounds were selected based on the following criteria: at least two consecutive concentrations significantly protected Antigen 18A from aggregation at air-liquid interface,

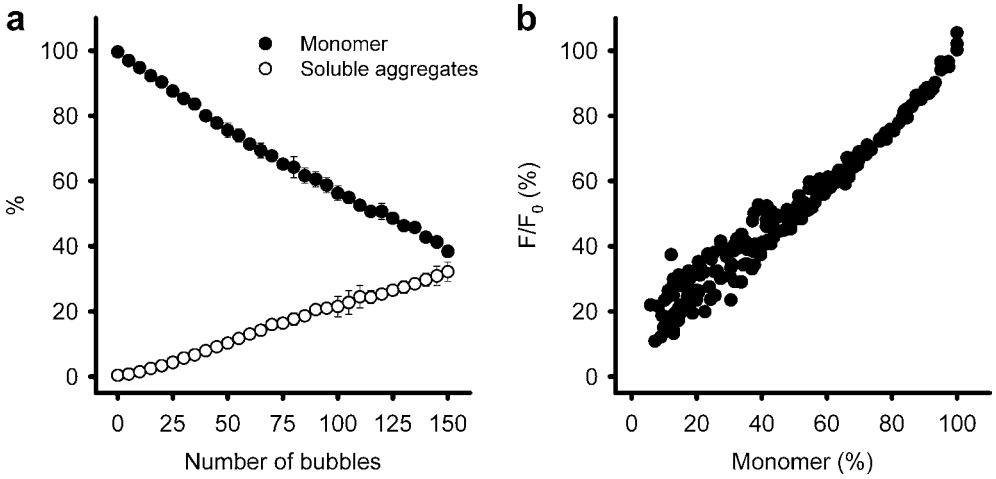

Fig. 6 Influence of air-liquid interface on Antigen 18A aggregation profile by size-exclusion chromatography and tryptophan fluorescence spectroscopy. Air-liquid interface was created by air bubbling in microplate. (**a**) Evolution of monomer and soluble aggregate species upon air bubbling. *Error bars* represent the standard deviation from three independent experiments. (**b**) Comparison of size-exclusion chromatography and tryptophan fluorescence spectroscopy for measuring Antigen 18A stability.

and at least one of them had a F/F_0 value greater than 80%. Hit excipients were the seven following compounds: hydroxypropyl-β-cyclodextrin, hydroxypropyl-γ-cyclodextrin, poloxamers 188 and 407, polysorbates 20 and 80, and Myrj 52. No significant effect of any hit excipient on pH was observed ($p>0.01$).

Based on the 72 excipient-free controls, the repeatability (intraplate), reproducibility (interplate) and global variability (intraplate + interplate) were estimated to be 12%, 7% and 13%, respectively. No significant row or column effect was observed ($p>0.01$).

In order to evaluate the feasibility of identifying hit excipients by this HTS method, we calculated a z'-value post-screening. This adimensional statistical parameter gives an idea of the width of the screening window (34). From the screening results (Fig. 7), we selected the positive (PX 188 0.125%) and negative (PVP K17 0.25%) controls based on a significant protection or destabilization of Antigen 18A at air-liquid interface, respectively. A plate was filled with positive and negative controls, in the same configuration as in the screening, i.e. blanks were placed on outer rows and all conditions were randomized on the plate. The samples were then submitted to air bubbling. Results are presented on Fig. 8. We obtained the following F/F_0 results: 94±2% for positive controls and 59±3% for negative controls. The calculated z'-value was 0.57, making the identification of excipient hits by this HTS method feasible (34).

Confirmation of the Performance of Hit Excipients

The performance of the seven hit excipients was further studied in half-filled vials. A shaking time of 1 h 30 min was applied (44±6% monomer loss) in order to meet conditions similar to the 100 bubbles used in the HTS study (44±2% monomer loss). Results of SEC analyses are presented in Fig. 9a. Significant protection of Antigen 18A ($p<0.05$) was observed with both cyclodextrins at 10% and with all surfactants from 0.015%.

Based on SEC results, a concentration of 10% for hydroxypropylcyclodextrins and 0.015% for surfactants was selected for further characterization. ELISA was used to assess the integrity of Antigen 18A epitopes after 1 h 30 min of shaking in vials in the presence of excipient candidates. Results are presented in Fig. 9b. After 1 h 30 min of shaking, hydroxypropylcyclodextrins and poloxamers significantly protected Antigen 18A from aggregation at air-water interface ($p<0.05$).

DISCUSSION

Aggregation in the Presence of Air-Liquid Interface

SEC analyses showed a progressive degradation of Antigen 18A monomer and the formation of soluble aggregates upon shaking in a half-filled vial (Fig. 1) or submission to air bubbles in a microplate (Fig. 6a). In both stress conditions, a simple mass balance calculation showed a progressive decrease in protein recovery. A loss of protein material could be explained by the presence of insoluble aggregates that are not detected by size-exclusion chromatography. This hypothesis is supported by a total disappearance of monomer and soluble aggregate species by SEC with harsher shaking protocols even if no particle was detected by visual observation (data not shown). While SEC is often considered as the standard reference for studying protein aggregation, this separation technique has potential limitations, e.g. interactions with stationary phase, modifications of the aggregate profile due to pressure or sample dilution, and loss of large particles on the chromatographic resin by filtration (40).

Spectroscopic and light scattering techniques were used to characterize Antigen 18A aggregation kinetics when

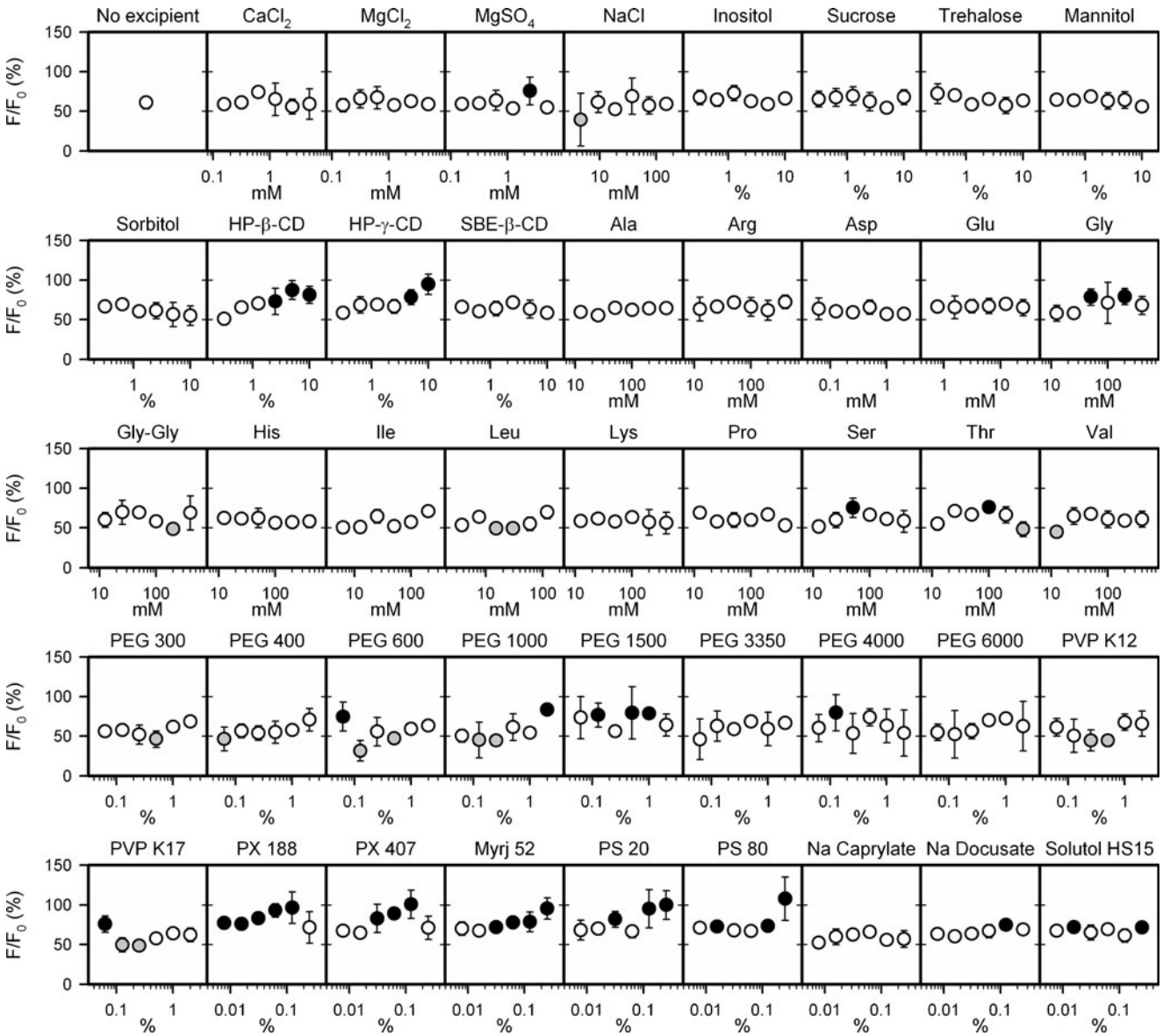

Fig. 7 High-throughput screening of excipients to prevent Antigen 18A aggregation at air-liquid interface, followed by tryptophan emission at 336 nm. A total of 100 air bubbles were used for creating air-liquid interface in microplate wells. *Closed symbols* represent conditions where statistically significant protection (*black*) or destabilization (*grey*) was noticed ($p < 0.01$) by ANOVA-Dunnett analysis. *Error bars* represent the standard deviation from three replicates randomly located on different plates.

shaken in a half-filled vial. Upon shaking, we measured an increase in β-sheet content (ATR-FTIR, Fig. 4), in the exposure of hydrophobic regions (Nile Red fluorescence spectroscopy, Fig. 3), and in aggregation (OD_{350} and RALS, Fig. 2).

Among all methods used in this aggregation kinetics study, Nile Red fluorescence revealed to be the most sensitive technique. By monitoring the position of the center of gravity of emission, we observed a significant increase in protein surface hydrophobicity after 30 min of shaking (Fig. 3c). Analyses by SEC were performed in parallel, and aggregation was significantly observed after 1 h of shaking. Nile Red fluorescence was already reported to have a higher sensitivity than SEC (36). The less discriminative techniques were light scattering methods. Aggregates were significantly detected after 2 h 15 min of shaking by RALS (Fig. 2a) and 3 h 30 min of shaking by OD_{350} (Fig. 2b). The superiority of RALS on OD_{350} could be due to the detector position. Whereas the latter is a transmission method, the detector is located at 90° in the former, which is more convenient for turbidity measurements.

These data suggest that conformational changes are involved in Antigen 18A aggregation at air-liquid interface. The use of complementary biophysical techniques was shown to be necessary for the characterization of protein aggregates (40). Indeed, while similar SEC profiles (Fig. 1a)

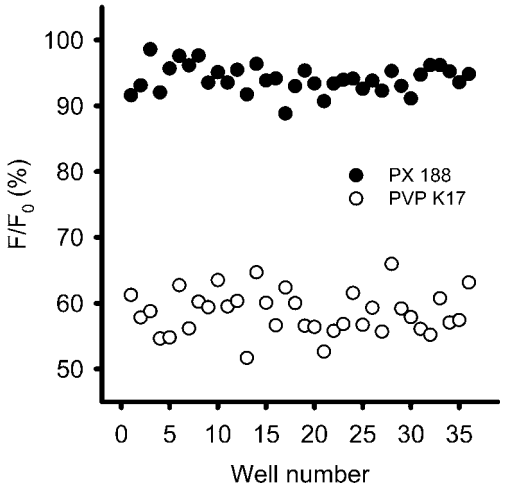

Fig. 8 Post-screening validation of the high-throughput screening assay. Controls were selected based on the HTS results, where significant protection (poloxamer 188 0.125%) or destabilization (polyvinylpyrrolidone K17 0.25%) of Antigen 18A against aggregation at air-liquid interface was noticed. Results were obtained from a single microplate.

were observed for aggregates obtained by shaking in a half-filled vial or by air bubbling in a microplate, fluorescence spectroscopy was able to detect some differences. For instance, tryptophan fluorescence spectroscopy detected significant changes upon air bubbling (Fig. 6b), while no differences were obtained upon shaking (data not shown). The opposite was true with Nile Red that detected significant differences upon shaking (Fig. 3) but not upon air bubbling (data not shown). Therefore, it was necessary to evaluate the performance of excipient candidates in both types of stress conditions.

High-Throughput Screening of Excipients

Early development of a vaccine formulation is often driven by a low availability of antigen material and short deadlines. Therefore, in a classical development, the number of excipients evaluated is limited. Surfactants are classically used in order to prevent protein adsorption at air-liquid interface and the resulting aggregation (10,12,16–23). In addition, a couple of studies report protein stabilization by adapting the formulation pH (7,9) or by adding excipients, e.g. cyclodextrins (10,15,19,24), amino acids (7–9), or sugars (6). Therefore, competition at interfaces but also conformational and colloidal stabilization can play a role in preventing protein aggregation at air-water interface.

HTS technologies are based on fast analyses and low sample volumes. A large number of conditions can be tested with a relatively small amount of antigen material. Moreover, each condition can be replicated in order to integrate a statistical approach in data interpretation. The excipients evaluated in this study were first selected based on their presence in marketed drugs for the parenteral route. While there is an urgent need for identifying new excipients from an academic point of view (41), using approved excipients limits development time by avoiding long and costly toxicological studies. Some excipient families were not included in this study, as their use was considered out of scope, e.g. antioxidants and preservatives. Also, some compounds were discarded in view of the adverse effects with which they are associated, considering that vaccines are most of the time used in a prophylactic context and intended to neonates. Finally, a non-exhaustive

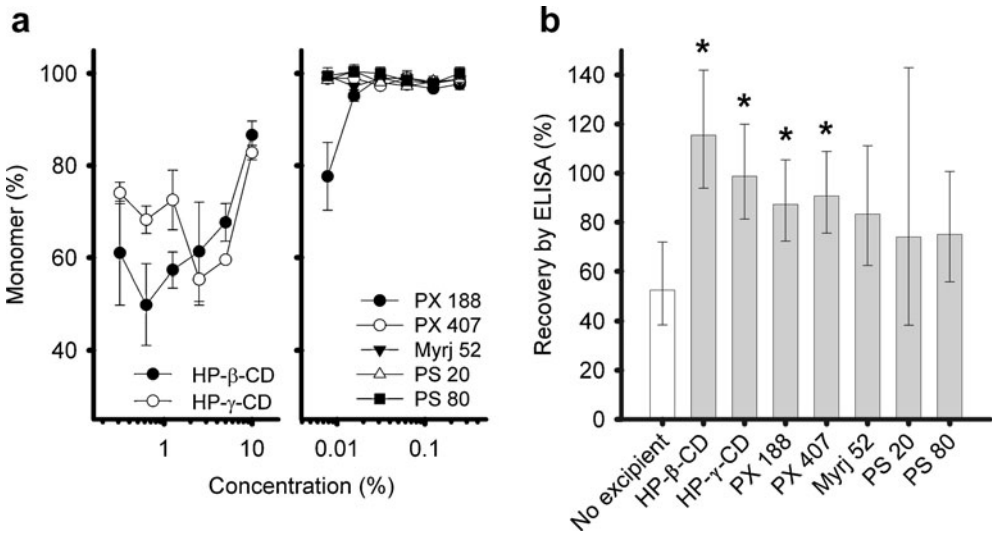

Fig. 9 Confirmation of the performance of excipient candidates in a shaken vial model. Agitation was performed during 1 h 30 min. (**a**) Monomer recovery by size-exclusion chromatography. *Error bars* represent the standard deviation from 3 independent experiments. (**b**) Integrity of Antigen 18A epitopes by enzyme-linked immunosorbent assay. Cyclodextrins and surfactants were added at a concentration of 10% and 0.015%, respectively. *Histogram bars* represent geometric means and their 95% confidence interval from five independent measurements. *Star symbols* indicate significant difference with the excipient-free control ($p < 0.05$) by ANOVA-Dunnett analysis.

list of 44 excipients was established, compatible with the liquid handler robot configuration used in this study. This excipient selection is convenient for studying the aggregation of a protein antigen irrespective of protein nature and stress test applied. We verified that the selected excipients did not interfere with the analytical methods used in this study.

The high sensitivity of fluorescence techniques (29) makes them very convenient to work at the low protein concentrations found in vaccines (typically lower than 1 mg/ml). Tryptophan fluorescence spectroscopy is a non-separative and label-free method, i.e. the sample is analyzed as such and no preparation is required. This technique was shown to be convenient for following Antigen 18A aggregation at 125 µg/ml (Fig. 6b). Combining tryptophan fluorescence spectroscopy with ultraviolet absorption spectroscopy in a multimode microplate reader allowed us to reliably measure the conformational changes of Antigen 18A in stress conditions and in the presence of various excipients (Fig. 7).

A major bottleneck in HTS is data management (26). While analyses are generally rapid, the thousands of figures generated by microplate readers can rapidly be overwhelming, and data management becomes a time-consuming operation. Each HTS process is different and requires the development of a customized application, based on the format of input and output files associated with equipments, plate layout, nature of analyses, calculations to be performed, and user requirements in terms of result display. In this study, we developed an integrated application used in the whole HTS process. Without any manual intervention from the generation of worklists used by the liquid handler robot up to the display of results, the risk of error was greatly reduced. Sample randomization in the plates increased objectivity. This approach allowed us to save time and to confidently interpret the HTS results.

The HTS evaluation of the 44 excipients revealed the performance of five surfactants and two cyclodextrins (Fig. 7). Protein protection by polysorbates (10,16–23), poloxamers (12) and hydroxypropylcyclodextrins (10,15,19,24) is already described in literature. Sulfobutylether-ethyl-cyclodextrin derivatives were also reported to have surfactant-like properties but were not included in this study because they are not used in any current commercial products (42). The amphiphilic nature of the surfactants but also of HP-β-CD (19) makes them good competitors for interfaces. These surface-active excipients could limit protein accessibility to air-water interfaces and therefore prevent adsorption-induced denaturation that triggers the aggregation process (2). A lower concentration of denatured species at interface may also limit irreversible interactions leading to the formation of aggregates. In addition, the protection conferred by an excipient could be possibly due to interactions with the protein (14,16) or to restriction in protein mobility due to an increase in viscosity. The question of protein stabilization mechanism by hit excipients was not addressed in this study. Using additional techniques including surface-tension and viscosity measurements would have been necessary for evaluating these different mechanistic approaches.

The critical micelle concentration (CMC) of a surfactant is the concentration from which micelles start to form. In absence of protein-surfactant interactions, protection by polysorbate 20 was reported to be maximal close to its CMC, independent of protein concentration (22). Another study showed protein stabilization by hydrophobic interactions with polysorbate 20 or 80 and protection below CMC, at surfactant:protein equimolar ratio (16). Therefore, both the nature of the surfactant and the nature of surfactant:protein interactions may play a role in protein protection from aggregation at air-liquid interface. As a rule of thumb, a monolayer of surfactant at interface should confer optimal protection, by using a concentration just above the excipient CMC (41). We observed that poloxamers 188 and 407 stabilized Antigen 18A at all concentrations, except the highest one (Fig. 7). A similar effect was shown to occur with polysorbate 80 (13). CMC values of 0.1% (25°C) and 0.095% (25.5°C) were found in literature for poloxamers 188 (43) and 407 (44), respectively. For both excipients, maximum protection was noticed at 0.125% ($p<0.01$), just above CMC, while no protection was observed at 0.250% ($p>0.01$). We postulate that Antigen 18A protection by poloxamers is concentration-dependent and that an optimum can be found close to the CMC.

Depending on the excipient:protein ratio, some additives revealed a beneficial or a detrimental effect on protein stability. Since the performance of an excipient can be related to its concentration, an HTS approach can be very convenient for simultaneously studying a large number of excipient:protein ratios. However, the efficient concentrations observed by tryptophan fluorescence in HTS (Fig. 7) were different from those observed by SEC in a shaken vial (Fig. 9a), probably due to differences in the nature of aggregates and to a lesser extent to the analytical method used (Fig. 6). These observations suggest that this HTS study of protein aggregation at air-liquid interface is convenient for identifying excipients but not for selecting excipient:protein ratios where the use of complementary biophysical techniques is required (40).

The performance of hydroxypropylcyclodextrins and poloxamers in protecting Antigen 18A from aggregation at air-liquid interface was confirmed in two different stress protocols. HP-β-CD at 0.35% was reported to be a valuable alternative to surfactants in inhibiting agitation-induced IgG aggregation (19). However, in the present study, adding 10% HP-β-CD or HP-γ-CD was necessary for observing a stabilizing effect on Antigen 18A, while aggregation was prevented by adding 0.015% poloxamer 188 or 407. At this concentration, a protective effect was

observed with poloxamers but not with polysorbates and Myrj 52 (Fig. 9b).

By identifying excipients known in the literature for stabilizing proteins against aggregation at air-liquid interface, the validity of the present HTS approach was confirmed. This objective strategy can find applications involving other analytical techniques, proteins and stress tests.

CONCLUSIONS

Antigen 18A was shown to denature in the presence of air-liquid interface and to form aggregates. We demonstrated the feasibility of identifying excipients for protecting this protein against aggregation at air-water interface by an HTS method. While amino acids, carbohydrates, polyols, polymers and salts appeared to be inefficient in that respect, some nonionic surfactants and hydroxypropylcyclodextrins were identified as performant excipient candidates. The superiority of poloxamers on polysorbates at protecting Antigen 18A was demonstrated.

Provided an integrated data management solution is available, HTS can be a powerful approach for evaluating the performance of excipients in protecting a protein antigen from aggregation. The high sensitivity of fluorescence methods makes them very convenient for working at low protein concentrations typical of vaccines. The case of Antigen 18A aggregation at air-liquid interface was presented but a similar HTS approach could be envisioned in other protein stability studies.

ACKNOWLEDGMENTS

This work was supported by GlaxoSmithKline Biologicals. The authors thank BASF, CyDex, Roquette and Sasol for providing gift samples of excipients, Laurent Bessemans and Caroline de Raikem for their support in programming the liquid handling robot, Carine Schroeders for technical assistance with ELISA analyses, Bénédicte Gbaguidi for advice with ATR-FTIR spectroscopy, the GlaxoSmithKline Biologicals R&D Media Preparation team for preparing excipient solutions, and Ulrike Krause and Pascal Cadot for their continuous support in reviewing the manuscript.

REFERENCES

1. Rathore N, Rajan RS. Current perspectives on stability of protein drug products during formulation, fill and finish operations. Biotechnol Prog. 2008;24(3):504–14.
2. Wang W. Protein aggregation and its inhibition in biopharmaceutics. Int J Pharm. 2005;289(1–2):1–30.
3. Hermeling S, Crommelin DJ, Schellekens H, Jiskoot W. Structure-immunogenicity relationships of therapeutic proteins. Pharm Res. 2004;21(6):897–903.
4. Hlady V, Buijs J, Jennissen HP. Methods for studying protein adsorption. Methods Enzymol. 1999;309:402–29.
5. Sluzky V, Tamada JA, Klibanov AM, Langer R. Kinetics of insulin aggregation in aqueous solutions upon agitation in the presence of hydrophobic surfaces. PNAS. 1991;88(21):9377–81.
6. Katakam M, Banga AK. Aggregation of insulin and its prevention by carbohydrate excipients. PDA J Pharm Sci Technol. 1995;49 (4):160–5.
7. Bringer J, Heldt A, Grodsky GM. Prevention of insulin aggregation by dicarboxylic amino acids during prolonged infusion. Diabetes. 1981;30(1):83–5.
8. Soenderkaer S, van de Weert M, Hansen LL, Flink J, Frokjaer S. Evaluation of statistical design/modeling for prediction of the effect of amino acids on agitation-induced aggregation of human growth hormone and human insulin. Drug Del Sci Tech. 2005;15:427–34.
9. Quinn R, Andrade JD. Minimizing the aggregation of neutral insulin solutions. J Pharm Sci. 1983;72(12):1472–3.
10. Charman SA, Mason KL, Charman WN. Techniques for assessing the effects of pharmaceutical excipients on the aggregation of porcine growth hormone. Pharm Res. 1993;10(7):954–62.
11. Maa YF, Hsu CC. Protein denaturation by combined effect of shear and air-liquid interface. Biotechnol Bioeng. 1997;54 (6):503–12.
12. Katakam M, Banga AK. Use of poloxamer polymers to stabilize recombinant human growth hormone against various processing stresses. Pharm Dev Technol. 1997;2(2):143–9.
13. Katakam M, Bell LN, Banga AK. Effect of surfactants on the physical stability of recombinant human growth hormone. J Pharm Sci. 1995;84(6):713–6.
14. Bam NB, Cleland JL, Yang J, Manning MC, Carpenter JF, Kelley RF, *et al.* Tween protects recombinant human growth hormone against agitation-induced damage via hydrophobic interactions. J Pharm Sci. 1998;87(12):1554–9.
15. Hagenlocher M, Pearlman R. Use of a substituted cyclodextrin for stabilization of solutions of recombinant human growth hormone. Pharm Res. 1989;6:S30.
16. Chou DK, Krishnamurthy R, Randolph TW, Carpenter JF, Manning MC. Effects of Tween 20 and Tween 80 on the stability of Albutropin during agitation. J Pharm Sci. 2005;94(6):1368–81.
17. Mahler HC, Muller R, Friess W, Delille A, Matheus S. Induction and analysis of aggregates in a liquid IgG1-antibody formulation. Eur J Pharm Biopharm. 2005;59(3):407–17.
18. Kiese S, Pappenberger A, Friess W, Mahler HC. Shaken, not stirred: mechanical stress testing of an IgG1 antibody. J Pharm Sci. 2008;97(10):4347–66.
19. Serno T, Carpenter JF, Randolph TW, Winter G. Inhibition of agitation-induced aggregation of an IgG-antibody by hydroxypropyl-beta-cyclodextrin. J Pharm Sci. 2010;99 (3):1193–206.
20. Thirumangalathu R, Krishnan S, Ricci MS, Brems DN, Randolph TW, Carpenter JF. Silicone oil- and agitation-induced aggregation of a monoclonal antibody in aqueous solution. J Pharm Sci. 2009;98 (9):3167–81.
21. Joshi O, Chu L, McGuire J, Wang DQ. Adsorption and function of recombinant Factor VIII at the air-water interface in the presence of Tween 80. J Pharm Sci. 2009;98(9):3099–107.
22. Kreilgaard L, Jones LS, Randolph TW, Frokjaer S, Flink JM, Manning MC, *et al.* Effect of Tween 20 on freeze-thawing- and agitation-induced aggregation of recombinant human factor XIII. J Pharm Sci. 1998;87(12):1597–603.
23. Wang W, Wang YJ, Wang DQ. Dual effects of Tween 80 on protein stability. Int J Pharm. 2008;347(1–2):31–8.

24. Banga AK, Mitra R. Minimization of shaking-induced formation of insoluble aggregates of insulin by cyclodextrins. J Drug Target. 1993;1(4):341–5.
25. Zhao H, Graf O, Milovic N, Luan X, Bluemel M, Smolny M, *et al.* Formulation development of antibodies using robotic system and High-Throughput Laboratory (HTL). J Pharm Sci. 2010;99 (5):2279–94.
26. Capelle MA, Gurny R, Arvinte T. A high throughput protein formulation platform: case study of salmon calcitonin. Pharm Res. 2009;26(1):118–28.
27. Ausar SF, Chan J, Hoque W, James O, Jayasundara K, Harper K. Application of extrinsic fluorescence spectroscopy for the high throughput formulation screening of aluminum-adjuvanted vaccines. J Pharm Sci. 2011;100(2):431–40.
28. Kyte J, Doolittle RF. A simple method for displaying the hydropathic character of a protein. J Mol Biol. 1982;157(1):105–32.
29. Lakowicz JR. Principles of fluorescence spectroscopy. New York: Springer; 2004.
30. McGown EL, Hafeman DG. Multichannel pipettor performance verified by measuring pathlength of reagent dispensed into a microplate. Anal Biochem. 1998;258(1):155–7.
31. Goormaghtigh E, Ruysschaert JM, Raussens V. Evaluation of the information content in infrared spectra for protein secondary structure determination. Biophys J. 2006;90(8):2946–57.
32. Kendrick BS, Dong A, Allison SD, Manning MC, Carpenter JF. Quantitation of the area of overlap between second-derivative amide I infrared spectra to determine the structural similarity of a protein in different states. J Pharm Sci. 1996;85 (2):155–8.
33. Oehlert GW. A first course in design and analysis of experiments. New York: W.H. Freeman & Co; 2000.
34. Zhang JH, Chung TD, Oldenburg KR. A simple statistical parameter for use in evaluation and validation of high throughput screening assays. J Biomol Screen. 1999;4(2):67–73.
35. Sackett DL, Wolff J. Nile red as a polarity-sensitive fluorescent probe of hydrophobic protein surfaces. Anal Biochem. 1987;167 (2):228–34.
36. Sutter M, Oliveira S, Sanders NN, Lucas B, van Hoek A, Hink MA, *et al.* Sensitive spectroscopic detection of large and denatured protein aggregates in solution by use of the fluorescent dye Nile red. J Fluoresc. 2007;17(2):181–92.
37. Byler DM, Susi H. Examination of the secondary structure of proteins by deconvolved FTIR spectra. Biopolymers. 1986;25 (3):469–87.
38. Dong A, Huang P, Caughey WS. Protein secondary structures in water from second-derivative amide I infrared spectra. Biochemistry. 1990;29(13):3303–8.
39. Pain RH. Determining the fluorescence spectrum of a protein. Curr Protoc Protein Sci. 2004;S38:7.7.1–7.7.20.
40. Carpenter JF, Randolph TW, Jiskoot W, Crommelin DJ, Middaugh CR, Winter G. Potential inaccurate quantitation and sizing of protein aggregates by size exclusion chromatography: essential need to use orthogonal methods to assure the quality of therapeutic protein products. J Pharm Sci. 2010;99(5):2200–8.
41. Jorgensen L, Hostrup S, Moeller EH, Grohganz H. Recent trends in stabilising peptides and proteins in pharmaceutical formulation - considerations in the choice of excipients. Expert Opin Drug Deliv. 2009;6(11):1219–30.
42. Samra HS, He F, Bhambhani A, Pipkin JD, Zimmerer R, Joshi SB, *et al.* The effects of substituted cyclodextrins on the colloidal and conformational stability of selected proteins. J Pharm Sci. 2010;99(6):2800–18.
43. Saski W, Shah SG. Availability of drugs in the presence of surface-active agents. I. Critical micelle concentrations of some oxyethylene oxypropylene polymers. J Pharm Sci. 1965;54:71–4.
44. Rassing J, Attwood D. Ultrasonic velocity and light-scattering studies on the polyoxyethylene-polyoxypropylene copolymer Pluronic F127 in aqueous solution. Int J Pharm. 1982;13(1):47–55.